RSC Advances

PAPER

View Article Online
View Journal | View Issue

Open Access Article. Published on 29 August 2023. Downloaded on 11/8/2025 10:45:24 AM.
This article is licensed under a Creative Commons Attribution-NonCommercial 3.0 Unported Licence.

Check for updates

Cite this: *RSC Adv.*, 2023, **13**, 25704

Bis(thienyl)ethenes with α-methoxymethyl groups. Syntheses, spectroscopic Hammett plots, and stabilities in PMMA films†

Thea Weingartz,[a] Sven Nagorny,[a] Jörg Adams,[b] André Eitzeroth,[b] Marvin Schewe,[c] Christian Rembe[c] and Andreas Schmidt *[a]

Received 3rd July 2023
Accepted 23rd August 2023

DOI: 10.1039/d3ra04444k

rsc.li/rsc-advances

A series of bis(thienyl)ethenes (BTEs) possessing perfluorocyclopentene backbones and methoxymethyl groups (MOM) in the 2/2′-positions of the thiophenes was prepared and examined. The substitution pattern of the 5/5′-positions was varied, covering the range from electron-donating to electron-withdrawing. The substituent effects of the absorption wavelengths of the ring-opened and the ring-closed isomers, which are interconverted by reversible 6π-electrocyclizations and cycloreversions, are studied by means of the spectroscopic Hammett equation and the Hammett–Brown equation. Excellent correlations of these linear free energy relationships were found, when the σ_p values of the Hammett equation, which summarize inductive, mesomeric and field effects, were replaced to the Hammett–Brown σ_p^+ and σ_p^- values which also take direct conjugation into account. We studied solvent effects on the spectroscopic properties and embedded the BTEs into polymethylmethacrylate (PMMA) coatings to examine their fatigue resistance. By our studies, the spectroscopic properties of BTEs can be adjusted by variation of the substitution pattern to a desired excitation wavelength for switching processes.

Introduction

The phenomenon of photochromism encompasses several reversible light-induced processes resulting in the formation of species which differ in their spectroscopic properties.[1] Photochromism can be based on reversible photoisomerism, or on the reversible formation of persistent radicals which reconstitute non-radical covalent forms. Some examples are shown in Scheme 1. *cis–trans* Isomerism causes the photochromism of azobenzenes **1**,[2] and structural isomerism results in photochromism of spiropyrans **2**,[3] furylfulgides **3**[4] and bis(thienyl) ethenes **4**.[1] Whereas the former reaction is a 6-*endo*-trig ring-closure under neutralization of the partial charges of the push–pull-chromophor, the two latter mentioned reactions are formal 6π-electrocyclizations to form ring-closed isomers. Punicines **5** and their derivatives are photochromic, because disproportionations produce radical cations and radical anions from the starting mesomeric betaine.[5] Among the examples shown, 1,2-bis(thienyl)ethenes (BTEs)[6] possessing perfluorocyclopentene backbones such as **4** undoubtedly are the most important. Depending on their substitution pattern they are thermally sufficiently stable and fatigue resistant,[7] and their response rate is considered fast enough for potential applications.[1] However, applications of BTEs usually require structural adjustments to find a compromise between desired absorption maxima for the switching processes and the other aforementioned properties. It is known that the C2/C2′ atoms of the thiophene rings of switchable BTEs need distances of 3.5–4.2 Å.[8] Through-space conjugation between these positions cause considerably shorter distances (3.28 Å),[9] which are also influenced by several other parameters such as the solvent polarity,[10] the constitution,[11] and substituent effects.[12] In order to use BTEs in films, absorbances, quantum yields, stabilities and photoactivities are the most important parameters, because some BTEs fail to undergo reversible photo-induced isomerisations when the solutions are too concentrated.[13] High concentrations of the dyes in the film, however, are desired to achieve high absorption contrasts. The 2-positions of the thiophene wings which are involved in the electrocyclization need to be substituted (R′ ≠ H) to prevent irreversible oxidations under formation of indeno[5,4-*b*:6,7-*b*′]dithiophenes **6** which are also described in a patent.[14] In addition, photochemical decompositions to form dithiacyclopenta[*a*]acenaphthylenes **7**[15] or 5-vinyl-indeno[5,4-*b*]thiophenes **8**[16] result in unfavourably low fatigue resistencies scheme 2.

[a]*Clausthal University of Technology, Institute of Organic Chemistry, Leibnizstrasse 6, D-38678 Clausthal-Zellerfeld, Germany. E-mail: schmidt@ioc.tu-clausthal.de*

[b]*Clausthal University of Technology, Institute of Physical Chemistry, Arnold-Sommerfeld-Straße 4, D-38678 Clausthal-Zellerfeld, Germany. E-mail: adams@pc.tu-clausthal.de*

[c]*Clausthal University of Technology, Institute for Electrical Information Technology, Leibnizstraße 28, D-38678 Clausthal-Zellerfeld, Germany*

† Electronic supplementary information (ESI) available: Hammett–Brown correlations, ^{1}H NMR, ^{13}C NMR and UV spectra. See DOI: https://doi.org/10.1039/d3ra04444k

© 2023 The Author(s). Published by the Royal Society of Chemistry

Open Access Article. Published on 29 August 2023. Downloaded on 11/8/2025 10:45:24 AM.
This article is licensed under a Creative Commons Attribution-NonCommercial 3.0 Unported Licence.

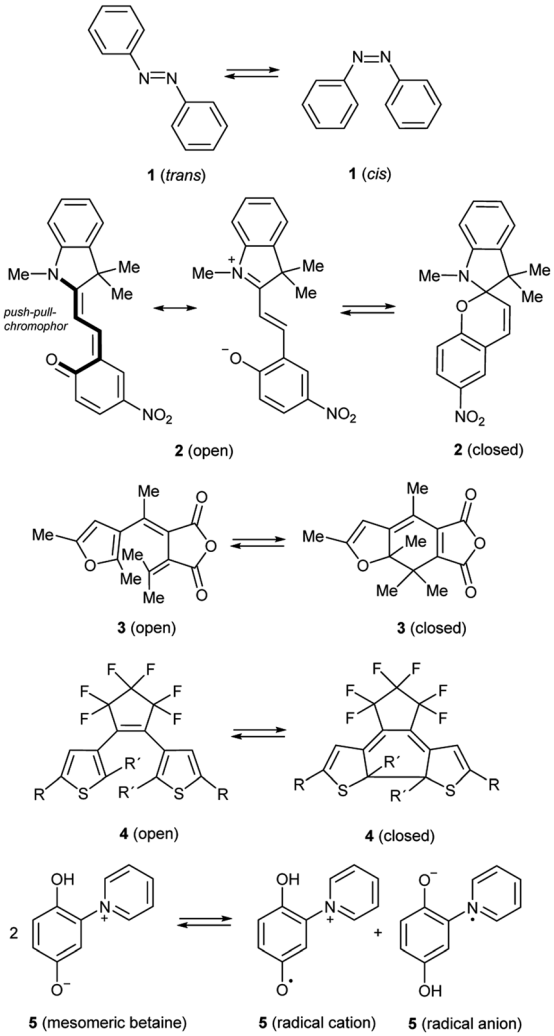

Scheme 1 Examples of photochromic molecules.

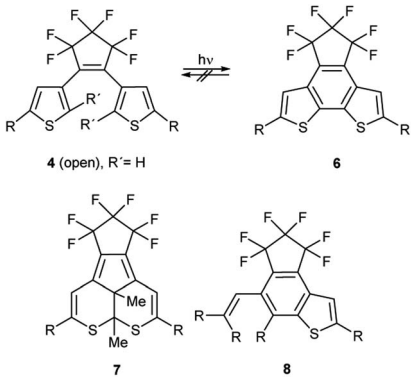

Scheme 2 Decomposition products of BTEs.

Only very few examples of BTEs which have other substituents than methyl groups in the 2-positions have been described to date.[17] We report here on the syntheses of BTEs with 2-methoxymethyl groups and various substituents in the 5-position, covering the range from electron-donating to electron-withdrawing. We found a linear free enthalpy relationship between the Hammett–Brown substituent constants of the substituents on the absorption maxima of the ring-opened as well as the closed form, when a modified spectroscopic Hammett equation is applied. Furthermore, we studied the behavior of the BTEs in polymethylmethacrylate (PMMA) films and examined their photoresistencies.

Results and discussion

The series of BTEs was prepared starting from 4-bromothiophene-2-carbaldehyde **9** and 3-bromothiophene **14** (Scheme 3). Thiophene **14** was used as a starting material for the synthesis of the unsubstituted reference BTE **15a** (X = H), and thiophene **9** served as starting material for the preparation of the BTEs **15b**, **15c**, **16**, **22**, and **23** with various substituents in their 5/5′-positions. First, 4-bromothiophene-2-carbaldehyde **9** was converted into the thiophene **10b** [X = Me, method (A)] in very good yield by Wolf–Kizhner reduction of the aldehyde group with hydrazine, and into **10c** [X = 1,3-dioxan-2-yl, method (B)] in almost quantitative yield by reaction with propanediol, respectively. Starting material **10b** was mentioned in the literature, however, no experimental procedure was described.[18] The formylation[19] of 3-bromothiophene **14** as well as of **10b,c** was

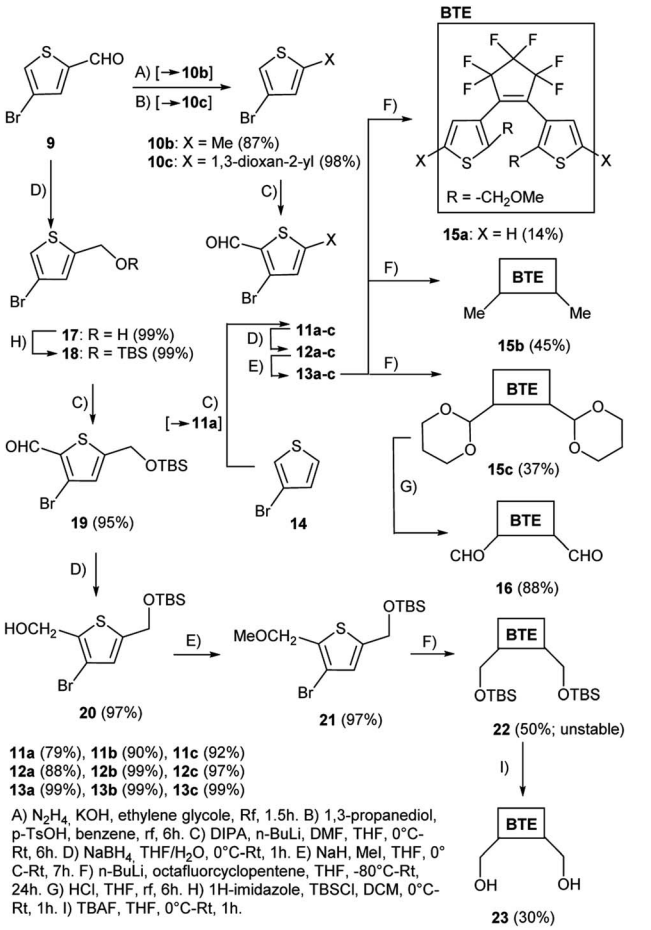

Scheme 3 Synthesis of the target BTEs.

Open Access Article. Published on 29 August 2023. Downloaded on 11/8/2025 10:45:24 AM.
This article is licensed under a Creative Commons Attribution-NonCommercial 3.0 Unported Licence.

performed under Vilsmeier–Haack conditions with lithium diisopropylamide and dimethylformamide [method (C)] to give **11a**, **11b**,[20] and **11c** in good to very good yields. Subsequent reduction to receive **12a–c** was performed applying sodium borohydride in a mixture of water and THF [method (D)] in yields between 88% and 99%. The methoxy derivatives **13a–c** were formed after treatment of **12a–c** with sodium hydride and iodomethane in quantitative yields, respectively [method (E)]. We found that an exchange of the solvent methanol[20] to THF reduced the reaction time considerably and increased the yields. The following reaction of **13a–c** with octafluorocyclopentene gave the target BTEs **15a–c** in low to moderate yields after bromide–lithium exchange with *n*-BuLi at −80 °C and substitution of fluorine of the substrate. Cleavage of the dioxane ring of **15c** was accomplished by HCl and resulted in the formation of BTE **16** in 88% yield [method (G)]. Starting material **21** for the preparation of the target BTEs **22** and **23** was synthesized over several steps starting from 4-bromothiophene-2-carbaldehyde **9** which was first subjected to a reduction with sodium borohydride to give **17** according to modified literature procedures[21] [method (D)], and then protected by a silyl group [method (H)][22] in quantitative yields, respectively. Performing the reaction under an inert atmosphere allowed a considerable shortened reaction time in comparison to the literature (1 h instead of 12 h[22]) and gave quantitative yields of thiophene **18**. Formylation to form thiophene-aldehyde **19** [method (C)], followed by reduction to give **20** was followed by methylation to yield **21**. The reaction of **21** with octafluorocyclopentene gave target BTE **22** in 50% yield. Because of the molecule's instability, the following reaction with TBAF [method (I)] was performed with a freshly prepared sample of **22** and gave BTE **23** in 30% yield.

The UV-vis absorption maxima of the 2-methoxymethyl-substituted BTEs described here measured in chloroform differ from those of the 2-methyl-substituted derivatives, as summarized in Table 1. All UV/vis absorption maxima of the open forms are slightly bathochromically shifted ($\Delta\lambda_{max} = -3.5$ to -9.2 nm) in comparison to the methyl analogs. The absorptions of the closed forms differ by −8.6 nm to +8.1 nm. Changing the solvent from $CHCl_3$ to THF causes shifts between −1.5 nm and −26.0 nm.

Table 1 Comparison of the UV/vis absorption maxima of the target BTEs possessing 2/2′-methoxymethyl groups and their 2/2′-methyl derivatives[27a]

		2/2′ = methoxymethyl		2/2′ = methyl
BTE		λ_{max} [nm] in THF	λ_{max} [nm] in $CHCl_3$	λ_{max} [nm] in $CHCl_3$
15a	Open	231.0	243.0	233.8
	Closed	511.0	519.0	514.0
15b	Open	214.0	242.0	n.d.[28]
	Closed	515.0	509.5	502.0
15c	Open	237.0	241.5	238.0
	Closed	532.0	528.0	528.0
16	Open	264.0	266.5	263.0
	Closed	604.0	605.5	613.6
22	Open	Not stable	n.d.	n.d.
	Closed	Not stable	n.d.	n.d.
23	Open	239.0	242.0	238.5
	Closed	519.0	525.5	516.9

[a] n.d. = not determined

In order to quantify the substituent effects in the 5-position on the spectroscopic properties, we performed Hammett correlations by means of the spectroscopic Hammett eqn 1, where R is the gas constant, T is the temperature, ρ_A is the absorption constant, and $E_{T,R}$ and $E_{T,H}$ are excitation energies of the substituted molecule and of its corresponding unsubstituted reference compound, respectively.[23] The constant σ is characteristic of a substituent,[24,25] and sum up the total electric effects such as inductive, mesomeric and field effects. These values were previously defined as substituents attached to substituted benzoic acids XC_6H_4COOH in *para*-position (σ_p) or *meta*-position (σ_m), the ionization of which was measured in water at 25 °C. The σ value is positive, when substituents exert electron-withdrawing properties on the ring, while negative values are indicative of electron-donating properties.[25]

$$\frac{E_{T,R} - E_{T,H}}{2303 \cdot R \cdot T} = \sigma\rho_A \tag{1}$$

The energies are calculated as follows from the spectra:

$$E_T = h \cdot c \cdot \tilde{\nu}_{max} \cdot N_A \tag{2}$$

Modified σ-values, σ^+ and σ^- values, have been introduced by H. C. Brown[26] for substituents which can enter into direct resonance interaction with the reaction site in the transition state. They were determined as rate constants of the nucleophilic substitution of cumyl chlorides in 90% acetone/water (σ_p^+) and from the deprotonation of substituted phenols as reference reaction (σ_p^-). The UV/vis-spectra of the BTEs described here were measured in tetrahydrofurane under identical conditions ($c = 0.05$ mg mL^{-1}) at rt and were used for the calculations of the excitation energies according to eqn 2 and Hammett as well as Hammett–Brown correlations according to eqn 1. Table 2 summarizes the results and the following Figures show the molar excitation energies plotted against the σ_p^+ and σ_p^- values of the different substituents. The value of the 1,3-dioxane-2-yl group was determined by us by application of the spectroscopic Hammett–Brown equation, as there is no constant available from the literature for this substituent.[27] As it can be seen from the UV/vis-spectra, the electron-withdrawing groups, *e.g.* –CHO, lead to a bathochromic shift and the electron-donating groups lead to a hypsochromic shift. This results in a negative absorption constant and a negative slope of the correlations. Hammett plots employing the original σ values gave correlations which were rated with "satisfactory" according to a rating system by Jaffé,[24c] as a coefficient of determination of 0.9689 was found for the closed forms (Fig. S1 and S2, ESI†). Using σ_p^+ values also resulted in satisfactory coefficients of determination of 0.9663 (Fig. 1). Employing Brown's σ_p^- values, however, gave an excellent correlation according to the aforementioned classification, as a coefficient of determination of 0.9989 was calculated (Fig. 2).

 © 2023 The Author(s). Published by the Royal Society of Chemistry

Open Access Article. Published on 29 August 2023. Downloaded on 11/8/2025 10:45:24 AM.
This article is licensed under a Creative Commons Attribution-NonCommercial 3.0 Unported Licence.

Table 2 Spectroscopic data for the Hammett and Hammett–Brown correlations (in $CHCl_3$)

BTE	substituent	λ_{max} [nm]	σ_p	σ_p^+	σ_p^-	Exc. energy [kJ mol^{-1}]
15a	H	243.0	0.00	0.00	0.00	492.29
		519.0				230.49
15b	Me	242.0	−0.17	−0.31	−0.17	494.32
		509.5				234.79
15c	1,3-Dioxan-2-yl	241.5	0.011	0.006	0.132	495.35
		528.0				226.57
16	CHO	266.5	0.42	0.73	1.03	448.88
		605.5				197.57
23	CH_2OH	242.0	0.00	−0.04	0.08	494.32
		525.5				227.64

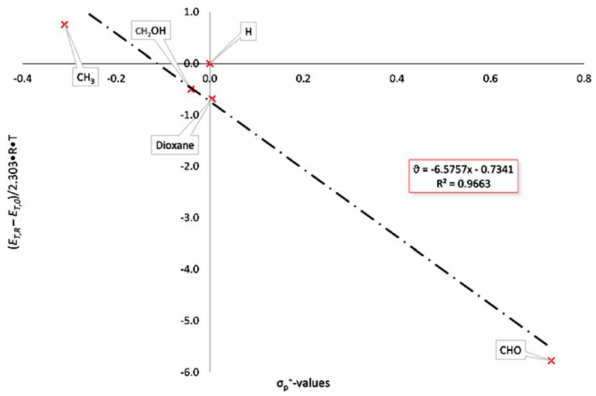

Fig. 1 Hammett–Brown correlation of the BTEs (closed form) applying σ_p^+ values.

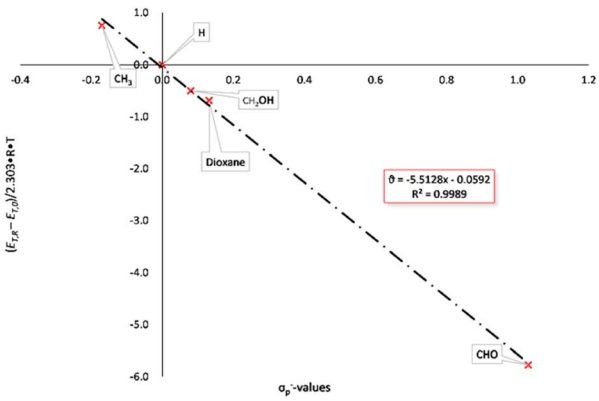

Fig. 2 Hammett–Brown correlation of BTEs (closed form) with σ_p^- values.

As expected, changing the solvent from chloroform (Table 2) to THF (Table 3) leads to different values of the absorption maxima of the open as well as of the closed state, and therefore also affects the excitation energies. Thus, higher excitation energies are necessary in THF in comparison to chloroform to switch the molecule into the closed form. The choice of solvent also influences the quality of the correlation coefficients and coefficients of determination of the Hammett and Hammett–Brown plots. Table 4 summarizes values achieved in THF, dichloromethane, chloroform, and methanol. These solvents not only differ in their solvent polarities, as expressed in their E_T^N values (CH_2Cl_2: 0.309; $CHCl_3$: 0.259; MeOH: 0.762; THF: 0.207),[23a] but also in their donicities and hydrogen bond donating properties. In contrast to DCM and chloroform, THF is an electron-pair-donating solvent (EPN solvent) which has a considerable donicity ($DN^N = 0.52$).[23a] Apart from the strongest polarity within this series of solvents we applied, methanol is a strong hydrogen-bond donating solvent. All Hammett and Hammett–Brown correlations of open and closed forms in the different solvents (THF, $CHCl_3$, CH_2Cl_2, MeOH) are shown in the ESI (Fig. S3–S24†). The correlations can be classified as "fair fit" when R is >0.90, "satisfactory" for $R > 0.95$ and "excellent" whenever R is >0.99).[24c] Table 4 summarizes correlation coefficients R and coefficients of determination R^2 for all measurements. As can be seen from Table 4, best correlation coefficients and coefficients of determination were achieved with chloroform as solvent.

To understand the effect of the methoxymethyl groups we compared the spectrocopic data with those of the reference compound shown in Scheme 4, which was prepared as described earlier.[27] Table 5 shows the quantum yields and the molar absorption coefficients. Comparing **15a** and the reference BTE reveals that the MOM group increases the molar absorption coefficient ε_A of the ring-opened form, whereas the quantum yields $\varphi_{A,B}$ decrease slightly. Best quantum yields $\varphi_{A,B}$ were achieved with molecule **15c** containing the 1,3-dioxan-2-yl rings and **23** possessing –CH_2OH substituents in the 5/5′-positions, and the best absorption coefficient with the dialdehyde BTE **16**. Interestingly, BTE **16** reaches a value of 49.4% quantum yield in the transferring process to the closed state, despite needing the lowest excitation energy compared to the other molecules.

As expected, the signals of the thiophenes in the ^{1}H NMR spectrum were shifted to smaller resonance frequencies δ, when the sample was irradiated (Table 6). Even after irradiation of the BTEs over a period of 8 h, it was not possible to convert them completely into their closed forms. As there were still signals of the open form in all cases, it was only possible to determine the conversion rate using the same irradiation time. As already mentioned, BTE **16** had the highest conversion during this experiment. The BTEs **15b** and **15c** reached the same conversion

Open Access Article. Published on 29 August 2023. Downloaded on 11/8/2025 10:45:24 AM.
This article is licensed under a Creative Commons Attribution-NonCommercial 3.0 Unported Licence.

Table 3 Spectroscopic data for the Hammett and Hammett–Brown correlations (in THF)

BTE	Substituent	λ_{max} [nm]	σ_p	σ_p^+	σ_p^-	Exc. energy [kJ mol^{-1}]
15a	H	231.8	0.00	0.00	0.00	516.08
		510.2				234.47
15b	Me	236.1	−0.17	−0.31	−0.17	506.68
		511.2				243.01
15c	1,3-Dioxan-2-yl	235.0	0.011	0.006	0.132	509.05
		532.0				224.86
16	CHO	264.4	0.42	0.73	1.03	452.10
		600.6				199.18
23	CH_2OH	237.8	0.00	−0.04	0.08	503.06
		517.0				231.39

Table 4 Correlation coefficients and coefficients of determination of all spectroscopic Hammett and Hammett–Brown plots in the used solvents

	Solvent			
σ_p	THF	$CHCl_3$	DCM	MeOH
σ_p Open	$R = 0.9073$	$R = 0.9392$	$R = 0.9226$	$R = 0.9170$
	$R^2 = 0.8232$	$R^2 = 0.8821$	$R^2 = 0.8511$	$R^2 = 0.8409$
σ_p Closed	$R = 0.9494$	$R = 0.9843$	$R = 0.9540$	$R = 0.9579$
	$R^2 = 0.9013$	$R^2 = 0.9689$	$R^2 = 0.9102$	$R^2 = 0.9175$
σ_p^+ Open	$R = 0.9039$	$R = 0.9429$	$R = 0.9126$	$R = 0.9081$
	$R^2 = 0.8171$	$R^2 = 0.8890$	$R^2 = 0.8328$	$R^2 = 0.8246$
σ_p^+ Closed	$R = 0.9496$	$R = 0.9830$	$R = 0.9561$	$R = 0.9606$
	$R^2 = 0.9018$	$R^2 = 0.9663$	$R^2 = 0.9141$	$R^2 = 0.9228$
σ_p^- Open	$R = 0.9546$	$R = 0.9647$	$R = 0.9581$	$R = 0.9513$
	$R^2 = 0.9112$	$R^2 = 0.9306$	$R^2 = 0.9179$	$R^2 = 0.9050$
σ_p^- Closed	$R = 0.9836$	$R = 0.9994$	$R = 0.9857$	$R = 0.9866$
	$R^2 = 0.9674$	$R^2 = 0.9989$	$R^2 = 0.9716$	$R^2 = 0.9734$

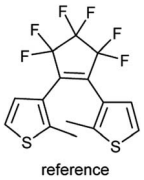

Scheme 4 Reference BTE.

Table 5 Wavelengths and quantum yields for the synthesized BTEs (in THF)[a]

BTE	$\lambda_{max,UV}$ [nm]	$\varphi_{A,B}$ [%]	$\varepsilon_A/10^3$	$\lambda_{max,Vis}$ [nm]	$\varphi_{B,A}$	$\varepsilon_B/10^3$
15a	231.8	56.7	15.11	510.2	0.1004	2.30
15b	236.1	50.9	19.78	511.2	0.0596	3.72
15c	235.0	66.4	18.52	532.0	0.0720	2.99
16	264.4	49.4	27.48	600.6	0.0129	3.13
23	237.8	61.8	16.69	517.0	0.0736	4.31
Ref.	233.1	55.3	11.86	512.4	0.2362	3.29

[a] These spectra were measured in THF with a concentration of 0.025 g mol^{-1} $\varepsilon/10^3$ is given in [L mol^{-1} cm^{-1}].

rate of 38%, whereas the BTEs **15a** and **23** have lower conversion rates of 21% and 28%.

In the next step we determined the effect of a polymethyl methacrylate (PMMA) matrix on the spectroscopic properties of the embedded BTEs and on their stabilities. PMMA is a preferred polymer to form matrices because of its high transparency and photostability.[29] The films were formed on a quartz surface by spin coating. The rotation speed was varied to adjust the thickness of the film, and UV/vis measurements confirmed the correlation between the film thickness and their absorptions. The thickness of the films was determined by confocal laser scanning microscopy (CLSM), which scanned an artificial scratch on the surface of the film by a laser to determine the distance between film surface and quartz surface. The software uses a method, where two points are set across the scratch with an average of 100 lines to determine the film thickness. For the films produced at 2500 rpm, the CLSM method gave a thickness of 400 nm, whereas a higher rotation speed of 3000 and 3500 rpm gave thinner films. The results of the stability tests in PMMA matrices of selected BTEs are shown below. The corresponding test setup is described in the experimental section. Fig. 3 shows a cyclization of BTE **15c** over 99 cycles. We used a yellow laser with 565 nm for the measurement and a reset beam, and a UV laser with 365 nm to induce the 6π-electrocyclization. For this kind of measurement a mixture of 3 mg of the corresponding BTE and 9 mg of solid PMMA was dissolved in 44.5 μL anisol which corresponds to a solid concentration of 24%.

Table 6 Conversion and shift of the aromatic protons (in $CDCl_3$)[a]

BTE	δ_{arom} (open) [ppm]	δ_{arom} (closed) [ppm]	Conversion [%]
15a	7.38 (d)	7.04 (d)	21
	7.12 (d)	6.32 (d)	
15b	6.77 (s)	6.06 (s)	38
15c	7.11 (s)	6.37 (s)	38
16	7.73 (s)	7.01 (s)	45
23	6.98 (s)	6.29 (s)	28

[a] The NMR-spectra were measured in $CDCl_3$ and the samples were irradiated at 254 nm for 2 h with a mercury lamp.

 © 2023 The Author(s). Published by the Royal Society of Chemistry

Open Access Article. Published on 29 August 2023. Downloaded on 11/8/2025 10:45:24 AM.
This article is licensed under a Creative Commons Attribution-NonCommercial 3.0 Unported Licence.

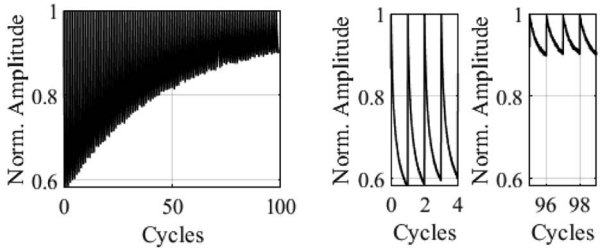

Fig. 3 Measured light power normalized to 1 as a function of the transmitted laser power over 99 cycles for BTE **15c**. One cycle is 3 s. Full plot (left) and two sections of 4 cycles at the start and at the end (right). Data is sampled with 5000 Hz and averaged over 10 samples.

The sections on the right in Fig. 3 show that the measured yellow laser power returns to a similar value at the start of each cycle. As the cycle progresses, the thin film gradually switches to the closed form and absorbs more yellow light, leading to a gradual decrease in the measured light power. However, after multiple cycles, an irreversible degradation of the dye molecules was observed, resulting in increasingly smaller changes in the measured light power.

Fig. 4 displays the absorptions of the examined BTEs, which can be determined from the negative decadic logarithm of the measured normalized light powers.

After around 35 cycles, the absorption of BTE **15c** has degraded by approximately 50%, while BTE **15a**, BTE **15b**, and BTE **23** take about 9, 10, and 15 cycles, respectively, to reach the same level of degradation. The absorption of the reference has degraded by 50% after around 22 cycles. As expected, BTE **16** shows a less stable behaviour as it degrades faster than the other BTEs and reaches 50% at already 6 cycles. Due to the electron-withdrawing effects of the aldehyde functions the system of BTE **16** becomes less stable. The comparison of BTE **15a** and the reference molecule shows that the methyl group of the reference has a stabilizing effect on the molecule system, as it degrades less fast. To increase the stability of this BTE system, different substituents can be introduced. As shown in Fig. 4, BTE **15c** with 1,3-dioxanyl substituents in 5-position reaches a degradation of 50% after approximately 35 cycles. This leads to a short conclusion that the 1,3-dioxan-2-yl substituents have a stabilizing effect on the molecule in comparison to the BTEs **15a** and BTE **23** containing a $-CH_2OH$ group is also more stable than the BTEs with only H and Me as substituents. It can be shown that the molecules are able to be stabilized by introducing electron-donating substituents.

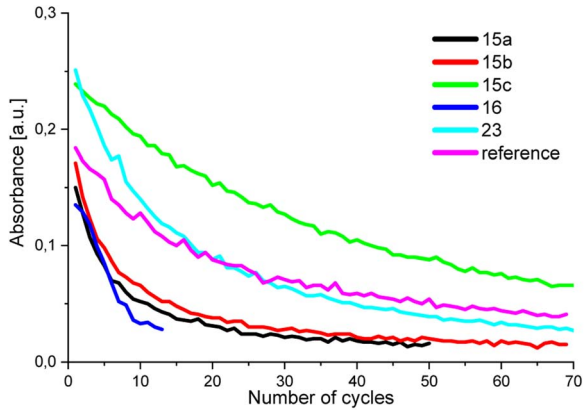

Fig. 4 Absorption of the BTEs in the closed form. The curves show a clear reduction in absorption due to degradation processes.

In summary we present first 2/2′-MOM-substituted bis(-thienyl)ethenes and linear free enthalpy relationships according the spectroscopic Hammett equation modified by Brown's substituent constants σ^+ and σ^-, which take direct conjugation into account. We examined the stabilities of these bis(thienyl) ethenes and found that the BTE with 1,3-dioxan-2-yl substituents in the 5/5′-positions and 2/2′-MOM groups is the most stable of the series in PMMA films.

Experimental section

General

All reactions were carried out under an atmosphere of nitrogen in oven-dried glassware. All chemicals were purchased and used without further purification unless otherwise mentioned. Anhydrous solvents were dried according to standard procedures before usage. Melting points were determined with a PerkinElmer DSC6. The ATR-IR spectra were obtained on a Bruker Alpha in the range of 400 to 4000 cm^{-1}. ^1H NMR spectra were recorded at 400 MHz or 600 MHz with a Bruker Avance/Avance III. ^{13}C NMR spectra were recorded at 100 MHz or 150 MHz, with the solvent peak used as the internal reference. Multiplicities are described by using the following abbreviations: s = singlet, d = doublet, t = triplet, and m = multiplet. Signal orientations in DEPT experiments were described as follows: o = no signal; + = up (CH, CH_3); − = down (CH_2). The electrospray ionization mass spectra (ESI-MS) were measured with a Bruker Impact-II mass spectrometer. Samples were sprayed from MeCN. Chromatography: The reactions were traced by thin layer chromatography with silica gel 60 (F254, MERCK KGAA). For the detection of substances, quenching was used at either 254 nm or 366 nm with a mercury lamp. The preparative column chromatography was conducted through silica gel 60 (230–400 mesh).

The films were produced on a quartz substrate with a size of 10 × 10 mm (1 mm thickness, PLANO). For the photostability measurements we used sapphire substrates (10.0 mm Ø, 1 mm thickness). For building up a matrix we used poly(methyl methacyrylate) (PMMA, average Mw 120 000 by GPC, SIGMA-ALDRICH), of which were dissolved 1000 mg in 10 mL of tetrahydrofurane (THF, 99.9%, anhydrous, inhibitor-free). The BTE (10 mg) was dissolved in 1 mL of THF (anhydrous, inhibitor-free, Sigma Aldrich). After evaporating of the THF, the different BTEs and PMMA were dissolved in anisole (99%, SIGMA-ALDRICH) within 1–7 days and these solutions were used for the coating of the quartz or sapphire substrate. As standard conditions we used 12% concentration of the solid, whereas the utilized ratio of BTE and PMMA was 50 : 50. For the photostability measurements we used a 24% solid concentration and a ratio of BTE and PMMA of 25 : 75. For producing the

Open Access Article. Published on 29 August 2023. Downloaded on 11/8/2025 10:45:24 AM.
This article is licensed under a Creative Commons Attribution-NonCommercial 3.0 Unported Licence.

coatings a Spin-coater (LAURELL WS-650 MZ-23MPP) was used. The produced coatings were investigated by using CLSM (Keyence VK-X210), for the scratch was used a canula (Sterican®, 0.40 × 20 mm). For taking pictures and determining the thickness was used the software "observation application".

The UV-vis spectra were recorded with the UV-vis-NIR spectrophotometer (type UV-670 JASCO GMBH, Germany), and the reviewed wavelengths were in the range of 200 and 800 nm. The baseline was recorded using solving-filled cuvettes as a reference. The concentration of the used solutions was 0.05 mg mL^{-1}. The used quartz cuvettes had a path length of 1 cm. Absorbance spectra of open and closed form derivatives were documented. For the switching procedure the light of a fluorescence spectrometer (FP-8500, JASCO) was used and guided *via* a liquid light guide (250-series, Lumatec) into the UV-vis-spectrometer. A self-made cell holder allows irradiate the solutions while simultaneously acquire spectra. The bandwidth of switching light was set to 5 nm, resulting in a light intensity of 0.5 mW.

To determine the quantum yields, the UV-vis-NIR spectrophotometer mentioned above was used. As solvent, THF (99.9%, anhydrous, inhibitor-free) was used. A concentration of 0.025 mg mL^{-1} was applied. The measurements concerning the switching process (transfer to the closed state) were done according to literature.[30] The quantum yields of the reverse reaction (close to open) were determined using a procedure described by Stranius and Börjesson.[31] For the irradiation process the setup described above was used with a bandwidth of irradiation of 2.5 nm (open to close) and 10 nm (close to open) and a light intensity of 0.5 mW. For the irradiation of molecule **16** was used a 3 watt LED (630–640 nm, Bridgelux/Epistar)

To determine the stabilities of the BTEs in films, we used a setup as shown in Fig. 5. We applied a yellow laser with a wavelength of 565 nm and a power of approx. 150 mW (MPB Communications 565 nm laser, Model F-04306-2) and a UV laser with a wavelength of 325 nm (Kimmon Koha HeCd Laser IK 3083 R-D). To control the intensity of the yellow laser, we employed a rotation stage with a half wave plate and a polarizing beamsplitter. An acousto-optic modulator (MQ110-A3-UV) is used to regulate the light power of the UV laser. A photosensor (Hamamatsu H10722-20 with 740 mV gain) is employed as detector, with an edge filter positioned in front to block UV light.

The beams were aligned using a pellicle beam splitter (BS) and positioned on the film by a mirror. An achromat is used to focus the beams to a diameter of approx. 200 μm.

A cycle consisted of two steps:

(I) Switching: the film was exposed to both the UV laser and the yellow laser simultaneously. The yellow laser power is set low enough to not interfere with the switching to the closed form. During this process, the absorption for yellow light increases, and the detected power decreases. For this switching process, the UV laser power on the target was set to approx. 0.5 mW and the yellow laser power was set to 10 μW for 2 s. To measure only the yellow laser power, an edge filter is used to block most of the UV laser power.

(II) Reset, the film is illuminated only by the yellow laser to reverse the switching process to the open form. A high laser power of about 10 mW is used for 4 seconds. During the reset, the switching process is almost completely reversed. The detected laser power at the beginning of each cycle is therefore approximately the same. To determine the photostationary state, the film was exposed to UV light until the transmitted yellow laser power was nearly constant and did not decrease further. This time T_{max} is defined as the time to fully complete the switching process. A switching time of about 90% of T_{max} is then selected for the cyclization. Note that the aforementioned times were specified for BTE **15a** and BTE **15b**. For BTE **15c** and BTE **23** 6 seconds to reset and 3 seconds for the switching was used, while the laser powers were the same.

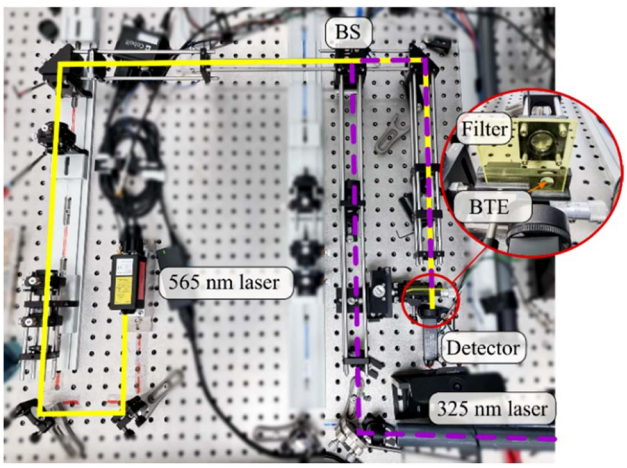

Fig. 5 Experimental setup for the determineation of stabilities. The yellow and UV laser are superimposed by a beam splitter (BS) and focused on the film by a lens. The transmitted yellow light is detected by a detector, while the transmitted UV light is blocked by an edge filter.

General procedure for the formylation [method (C)]

Diisopropylamine (1.2 eq.) was dissolved in 30 mL of anhydrous THF. At 0 °C was slowly added *n*-butyllithium (24% in cyclohexane, 1.1 eq.). The reaction mixture was stirred at this temperature for 45 min. The thiophene derivative (1.0 eq.) was dissolved in 10 mL of anhydrous THF and added to the reaction mixture at 0 °C. The reaction was stirred for 30 min at this temperature and then three hours at room temperature. The reaction was then quenched with 40 mL of a saturated ammonium chloride solution. The aqueous phase was extracted two times with 50 mL of diethyl ether. The organic phase was washed once with 20 mL of 1M HCl, two times with 50 mL of water, and dried over $MgSO_4$. Finally, the solvent was removed *in vacuo*.

General procedure for the synthesis of the alcohols [method (D)]

The aldehyde (1.0 eq.) was dissolved in a mixture of THF and water (10 : 1). At 0 °C, sodium borohydride (0.5 eq.) was slowly added. The reaction mixture was stirred for 30 min at 0 °C and another 30 min at room temperature. Afterwards the reaction

 © 2023 The Author(s). Published by the Royal Society of Chemistry

Open Access Article. Published on 29 August 2023. Downloaded on 11/8/2025 10:45:24 AM.
This article is licensed under a Creative Commons Attribution-NonCommercial 3.0 Unported Licence.

was quenched with 50 mL of water followed by an aqueous workup. The aqueous phase was extracted with 50 mL of diethyl ether (two times). The combined organic phases were washed with 100 mL of water (four times). Finally, the organic phase was dried over $MgSO_4$ and the solvent was removed *in vacuo*.

General procedure for the methylation [method (E)]

The alcohol was dissolved in 30 mL of anhydrous THF. Sodium hydride (60%, 1.1 eq.) was slowly added at 0 °C. Iodomethane (1.1 eq.) was then added after 50 min at 0 °C. The reaction mixture was stirred for 30 min at this temperature and another four hours at room temperature. The reaction was then quenched with 50 mL of water followed by an aqueous workup. The aqueous phase was extracted twice with 50 mL of diethyl ether, and the combined organic phases were washed three times with 50 mL of water. The organic phase was dried over $MgSO_4$ and the solvent was removed *in vacuo*.

General procedure for the synthesis of the BTEs [(method F)]

The reaction was carried out under a nitrogen atmosphere. 1 eq. of the halogenated thiophene was dissolved in anhydrous THF and the mixture was then cooled to −80 °C. To this solution 1.05 eq of a solution of 2.8 M *n*-BuLi in hexane was added. After 30 min, octafluorocyclopentene (0.5 eq.) was added in small portions over a period of 30 min. After 2 h the reaction was allowed to warm to room temperature and was then stirred overnight. A portion of 30 mL of water was then added to quench the reaction. The aqueous phase was extracted two times with 50 mL diethyl ether, and the organic phase was washed once with 20 mL of 1M HCl, and two times with 50 mL of water. Then, it was dried over $MgSO_4$ and the solvent was removed *in vacuo*. The crude product was purified by column chromatography to afford the BTEs.

Synthesis of BTE 15a

3-Bromothiophene-2-carbaldehyde (11a). According to method (C) 5.17 mL (36.80 mmol) of DIPA, 13.20 mL (33.73 mmol) of *n*-BuLi (24% in cyclohexane), 2.87 mL (30.66 mmol) of 3-bromothiophene **14** and 2.83 mL (36.80 mmol) of DMF were reacted. Yield 4.616 g (79%), yellow liquid. ^{1}H NMR ($CDCl_3$, 400 MHz): $\delta = 9.98$ (s, 1H, H6), 7.71 (d, $J = 5.1$, 1.2 Hz, 1H, H5), 7.15 (d, $J = 5.1$, 1.2 Hz, 1H, H4) ppm. The spectroscopic data agree with the literature.[32]

(3-Bromothiophen-2-yl)methanol (12a). Following method (D) 4.616 g (24.16 mmol) of 3-bromothiophene-2-carbaldehyde **9** and 0.457 g (12.08 mmol) of sodium borohydride were reacted. Yield 4.120 g (88%), yellow liquid. ^{1}H NMR ($CDCl_3$, 400 MHz): $\delta = 9.98$ (s, 1H, H6), 7.71 (d, $J = 5.1$, 1.2 Hz, 1H, H5), 7.15 (d, $J = 5.1$, 1.2 Hz, 1H, H4) ppm. The spectroscopic data agree with the literature.[33]

3-Bromo-2-(methoxymethyl)thiophene (13a). According to method (E) 2.000 g (10.36 mmol) of (3-bromothiophene-2-yl) methanol **11a**, 0.497 g (12.40 mmol) of sodium hydride and 0.71 mL (11.39 mmol) of iodomethane were reacted. Yield 2.123 g (99%), dark brown liquid. ^{1}H NMR ($CDCl_3$, 400 MHz): $\delta = 7.28$ (d, $J = 5.3$ Hz, 1H, H5), 6.95 (d, $J = 5.3$ Hz, 1H, H3), 4.60 (s, 2H, H6), 3.42 (s, 3H, H7) ppm. ^{13}C NMR ($CDCl_3$, 100 MHz): $\delta = 135.7$ (o, C2), 130.1 (+, C4), 125.9 (+, C5), 110.0 (o, C3), 68.1 (−, C6), 58.1 (+, C7) ppm. IR (ATR): $\nu = 2953$, 2928, 2885, 2856, 1542, 1462, 1371, 1254, 1184, 1128, 1080, 1005, 939, 833, 775, 688, 667, 594, 567 cm^{-1}. HR-ESI-MS: calc. $[M]^+$: 350.0371, calc. $[M + Na^+]$: 373.0264; found $[M + Na^+]$: 373.0267 ($\Delta = 0.0003$).

3,3′-(3,3,4,4,5,5-Hexafluorocyclopent-1-ene-1,2-diyl)bis(2-(methoxymethyl)thiophene) (14a). Following method (F) 2.000 g (9.66 mmol) of 3-bromo-2-(methoxymethyl)thiophene **13a**, 4.17 mL (10.62 mmol) of *n*-BuLi (24% in cyclohexane) and 0.65 mL (4.83 mmol) of octafluorocyclopentene were reacted. Yield 0.285 g (14%), yellowish oil. ^{1}H NMR ($CDCl_3$, 600 MHz): $\delta = 7.38$ (d, $J = 5.2$ Hz, 2H, H5, H5′), 7.13 (d, $J = 5.2$ Hz, 2H, H4, H4′), 3.87 (s, 4H, H6, H6′), 3.18 (s, 6H, H7, H7′) ppm. ^{13}C NMR ($CDCl_3$, 150 MHz): $\delta = 144.4$ (o, C2, C2′) 136.3–136.0 (m, C8, C8′), 127.1 (+, C4, C4′), 126.2 (+, C5, C5′), 124.1 (o, C3, C3′), 117.9–114.1 (m, C9, C9′), 113.1–109.1 (m, C10), 68.1 (−, C6, C6′), 58.2 (+, C7, C7′) ppm. IR (ATR): $\nu = 2931$, 2827, 1450, 1338, 1272, 1190, 1127, 1085, 1030, 977, 914, 846, 716, 648, 577, 549, 489 cm^{-1}. HR-ESI-MS: calc. $[M]^+$: 716.2280, calc. $[M + Na^+]$: 739.2172; found $[M + Na^+]$: 739.2176 ($\Delta = 0.0004$).

Synthesis of BTE 15b

4-Bromo-2-methylthiophene (10b). 5.000 g (26.33 mmol) of 4-bromothiophene-2-carbaldehyde **9** were dissolved of 100 mL of diethylene glycole. Then, 3.88 mL (78.98 mmol) of hydrazine hydrate were added and the reaction mixture was stirred for 1.5 h under reflux temperature. A sample of 8.830 (157.97 mmol) of potassium hydroxide in 9 mL of water was added and the reaction mixture was heated until no gas evolution was observed. Then, an azeotropic distillation at 160 °C with water was performed, followed by an aqueous workup of the distillate. The distillate was diluted with 50 mL of DCM. The aqueous phase was extracted with 30 mL DCM (two times) and the combined organic phases were washed with 50 mL water (two times). The organic phase was dried over $MgSO_4$ and the solvent was removed *in vacuo*. Yield 4.068 g (87%), a lightly yellow liquid. ^{1}H NMR ($CDCl_3$, 400 MHz): $\delta = 6.98$ (d, $J = 1.2$ Hz, 1H, H5), 6.88–6.89 (m, 1H, H3), 2.47 (d, $J = 1.2$ Hz, 3H, H6) ppm. The spectroscopic data agree with the literature.[34]

3-Bromo-5-methylthiophene-2-carbaldehyde (11b). According to method (C) 0.47 mL (3.38 mmol) of diisopropylamine were dissolved in 15 mL of anhydrous THF. 1.95 mL (3.11 mmol) of *n*-BuLi were added. Then, 0.500 (2.82 mmol) of 4-bromo-2-methylthiophene and 0.26 mL (3.38 mmol) of DMF were added slowly. Yield 0.524 g (90%), yellow liquid. ^{1}H NMR ($CDCl_3$, 400 MHz): $\delta = 9.87$ (s, 1H, H7), 6.85 (d, $J = 1.0$ Hz, 1H, H4), 2.55 (d, $J = 1.0$ Hz, 3H, H6) ppm. The spectroscopic data agree with the literature.[20]

(3-Bromo-5-methylthiophen-2-yl)methanol (12b). Following method (D), the desired alcohol **12b** was obtained by reaction of 3-bromo-5-methylthiophene-2-carbaldehyde **11b** (0.524 g, 2.55 mmol) with sodium borohydride (0.048 g, 1.27 mmol). Yield 0.523 g (99%), a yellow-brown solid. ^{1}H NMR ($CDCl_3$, 400 MHz): $\delta = 6.62$ (m, 1H, H4), 4.71 (s, 2H, H7), 2.45 (s, 3H, H6) ppm. The spectroscopic data agree with the literature.[20]

Open Access Article. Published on 29 August 2023. Downloaded on 11/8/2025 10:45:24 AM. This article is licensed under a Creative Commons Attribution-NonCommercial 3.0 Unported Licence.

3-Bromo-2-(methoxymethyl)-5-methylthiophene (13b). According to method (E) 3.000 g (14.49 mmol) of (3-bromo-5-methylthiophene-2-yl)methanol **12b**, 0.811 g (20.28 mmol) of sodium hydride (60% in paraffine) and 0.99 mL (15.93 mmol) of iodomethane were reacted. Yield 3.184 g (99%), brown liquid. ^{1}H NMR ($CDCl_3$, 600 MHz): δ = 6.62 (m, 1H, H4), 4.52 (s, 2H, H7), 3.38 (s, 3H, H8), 2.45 (m, 3H, H6) ppm. ^{13}C NMR ($CDCl_3$, 150 MHz): δ = 140.4 (o, C5), 132.8 (o, C2), 127.8 (+, C4), 109.3 (o, C3), 67.8 (−, C7), 57.9 (+, C8), 15.5 (+, C6) ppm. IR (ATR): ν = 2921, 2853, 2820, 1543, 1447, 1367, 1321, 1280, 1170, 1088, 998, 949, 906, 814, 564, 491 cm^{-1}. HR-ESI-MS: calc. [M]$^+$: 219.9557, calc. [M + Na$^+$]: 242.9450; found [M + Na+]: 242.9426.

3,3′-(3,3,4,4,5,5-Hexafluorocyclopent-1-ene-1,2-diyl)bis(2-(methoxymethyl)-5-methylthiophene) (15b). According to method (F) 3.184 g (14.39 mmol) of 3-bromo-2-(methoxymethyl)-5-methylthiophene **13b**, 10.85 mL (17.28 mmol) of *n*-BuLi (15% in *n*-hexane) and 0.96 mL (7.19 mmol) of octafluorocyclopentente were reacted. Column chromatography (*n*-hexane) gave the product. Yield 1.464 g (45%), dark red oil. ^{1}H NMR ($CDCl_3$, 600 MHz): δ = 6.77 (s, 2H, H4, H4′), 3.83 (s, 4H, H7, H7′), 3.15 (s, 6H, H8, H8′), 2.47 (s, 6H, H6, H6′) ppm. ^{13}C NMR ($CDCl_3$, 150 MHz): δ = 141.7 (o, C2, C2′), 140.6 (o, C5, C5′), 136.0 (m, o, C9, C9′), 124.6 (+, C4, C4′), 124.1 (o, C3, C3′), 117.6–114.2 (m, o, C10, C10′), 111.0–110.8 (m, o, C11), 67.9 (−, C7, C7′), 57.9 (+, C8, C8′), 15.3 (+, C6, C6′) ppm. IR (ATR): ν = 2987, 2926, 2824, 1738, 1633, 1494, 1449, 1336, 1268, 1190, 1126, 1093, 1060, 1025, 984, 912, 851, 823, 738, 683, 647, 586, 547, 502 cm^{-1}. HR-ESI-MS: calc. [M]$^+$: 456.0652, calc. [M + Na$^+$]: 479.0550; found. [M + Na+]: 479.0539.

Synthesis of BTE 15c

2-(4-Bromothiophen-2-yl)-1,3-dioxane (10c). A sample of 3.000 g (15.70 mmol) of 4-bromothiophene-2-carbaldehyde **9** was dissolved in 100 mL of benzene. 1.80 mL (25.14 mmol) of 1,3-propanediole and 0.270 g (1.57 mmol) of *p*-toluenesulfonic acid were added. The reaction mixture was refluxed for eight hours. After completion of the reaction (TLC control) the solvent was removed *in vacuo*. The residue was diluted with 30 mL of diethyl ether and washed with 50 mL of water (four times). The organic phase was dried over $MgSO_4$ and the solvent was removed. Yield 3.834 g (98%), slightly yellow liquid. ^{1}H NMR ($CDCl_3$, 600 MHz): δ = 7.18 (m, 1H, H5), 7.03 (m, 1H, H3), 5.67 (s, 1H, H6), 4.25–4.22 (m, 2H, H7$_{eq}$, H9$_{eq}$), 3.98–3.93 (m, 2H, H7$_{ax}$, H9$_{ax}$), 2.24–2.16 (m, 1H, H8$_{eq}$), 1.46–1.43 (m, 1H, H8$_{ax}$) ppm. ^{13}C NMR ($CDCl_3$, 150 MHz): δ = 142.8 (o, C2), 127.7 (+, C3), 122.9 (+, C5), 109.2 (o, C4), 97.5 (+, C6), 67.3 (−, C7, C9), 25.4 (−, C8) ppm. IR (ATR): ν = 3104, 2968, 2926, 2854, 1733, 1539, 1459, 1436, 1370, 1322, 1276, 1236, 1217, 1167, 1146, 1094, 1015, 977, 943, 925, 873, 860, 826, 737, 639, 586, 471 cm^{-1}. HR-ESI-MS: calc. [M]$^+$: 247.9507, calc. [M + Na$^+$]: 270.9404; found [M + Na$^+$]: 270.9392.

3-Bromo-3-(1,3-dioxan-2-yl)thiophene-2-carbaldehyde (11c). According to method (C) 2.03 mL (14.45 mmol) of DIPA, 8.32 mL (13.25 mmol) of *n*-BuLi, 3.000 g (12.04 mmol) of 2-(4-bromothiophen-2-yl)-1,3-dioxane **10c** and 1.12 mL (14.45 mmol) of DMF were reacted. Yield 3.074 (92%), yellow solid. Mp.: 91 °C. ^{1}H NMR ($CDCl_3$, 600 MHz): δ = 9.92 (s, 1H, H10), 7.13 (d, J = 0.8 Hz, 1H, H4), 5.65 (s, 1H, H6), 4.24–4.21 (m, 2H, H7$_{eq}$, H9$_{eq}$), 3.97–3.93 (m, 2H, H7$_{ax}$, H9$_{ax}$), 2.21–2.15 (m, 1H, H8$_{eq}$), 1.47–1.44 (m, 1H, H8$_{ax}$) ppm. ^{13}C NMR ($CDCl_3$, 150 MHz): δ = 183.2 (+, C10), 151.1 (o, C5), 136.5 (o, C2), 129.4 (+, C4), 119.5 (o, C3), 96.9 (+, C6), 67.3 (−, C7, C9), 25.3 (−, C8) ppm. IR (ATR): ν = 3089, 2994, 2980, 2963, 2935, 2882, 1659, 1525, 1461, 1433, 1360, 1344, 1317, 1281, 1238, 1202, 1156, 1143, 1087, 1046, 1018, 975, 950, 923, 898, 880, 851, 796, 692, 664, 643, 606, 561, 488, 470 cm^{-1}. HR-ESI-MS: calc. [M]$^+$: 275.9456, calc. [M + Na$^+$]: 298.9353; found [M + Na$^+$]: 298.9346.

(3-Bromo-5-(1,3-dioxan-2-yl)thiophene-2-yl)methanol (12c). Following method (E) 3.000 g (10.83 mmol) of 3-bromo-5-(1,3-dioxane2-yl)thiophene-2-carbaldehyde **11c** and 0.205 g (5.41 mmol) of sodium borohydride were reacted. Yield 2.924 g (97%), slightly brown solid. Mp.: 49 °C. ^{1}H NMR ($CDCl_3$, 600 MHz): δ = 6.96 (d, J = 0.7 Hz, 1H, H4), 5.64 (s, 1H, H6), 4.73 (s, 2H, H10), 4.24–4.21 (m, 2H, H7$_{eq}$, H9$_{eq}$), 3.97–3.93 (m, 2H, H7$_{ax}$, H9$_{ax}$), 2.22–2.16 (m, 1H, H8$_{eq}$), 1.46–1.42 (m, 1H, H8$_{ax}$) ppm. ^{13}C NMR ($CDCl_3$, 150 MHz): δ = 141.3 (o, C5), 138.5 (o, C2), 127.8 (+, C4), 107.9 (o, C3), 97.5 (+, C6), 67.2 (−, C7, C9), 59.2 (−, C10), 25.4 (−, C8) ppm. IR (ATR): ν = 3389, 2967, 2927, 2857, 1546, 1459, 1427, 1371, 1314, 1276, 1236, 1215, 1146, 1129, 1088, 1047, 1006, 978, 943, 923, 893, 859, 837, 746, 668, 640, 599, 473 cm^{-1}. HR-ESI-MS: calc. [M]$^+$: 277.9612, calc. [M + Na$^+$]: 300.9510; found [M + Na$^+$]: 300.9507.

2-(4-Bromo-5-(methoxymethyl)thiophen-2-yl)-1,3-dioxane (13c). Following method (E) 2.000 g (7.16 mmol) of (3-bromo-5-(1,3-dioxane-2yl)thiophene-2-yl)methanol **12c**, 0.401 g (10.03 mmol) of sodium hydride (60% in paraffine) and 0.49 mL (7.88 mmol) of iodomethane were reacted. Yield 2.080 g (99%), slightly brown liquid. ^{1}H NMR ($CDCl_3$, 600 MHz): δ = 6.98 (d, J = 0.7 Hz, 1H, H3), 5.64 (s, 1H, H8), 4.56 (s, 2H, H6), 4.24–4.21 (m, 2H, H9$_{eq}$, H11$_{eq}$), 3.97–3.92 (m, 2H, H9$_{ax}$, H11$_{ax}$), 3.37 (s, 3H, H7), 2.24–2.15 (m, 1H, H10$_{eq}$), 1.46–1.42 (m, 1H, H10$_{ax}$) ppm. ^{13}C NMR ($CDCl_3$, 150 MHz): δ = 141.7 (o, C2), 135.8 (o, C5), 127.8 (+, C3), 109.4 (o, C4), 96.7 (+, C8), 67.9 (−, C6), 67.3 (−, C9, C11), 58.0 (+, C7), 25.5 (−, C10) ppm. IR (ATR): ν = 2925, 2854, 1547, 1459, 1428, 1370, 1314, 1276, 1215, 1191, 1146, 1091, 1003, 974, 944, 925, 906, 835, 640, 604, 473 cm^{-1}. HR-ESI-MS: calc. [M]$^+$: 291.9769, calc. [M + Na$^+$]: 314.9661; found [M + Na$^+$]: 314.9668.

2,2′-((3,3,4,4,5,5-Hexafluorocyclopent-1-ene-1,2-diyl)bis(5-(methoxymethyl)thiene-4,2-diyl))bis(1,3-dioxane) (15c). According to method (F) 2.104 g (7.18 mmol) of 2-(4-bromo-5-(methoxymethyl)thiophen-2-yl)-1,3-dioxane **13c**, 5.41 mL (8.61 mmol) of *n*-BuLi (15% in *n*-hexane) and 0.48 mL of octafluorocyclopentene were reacted. Yield 0.788 g (37%), dark red oil. ^{1}H NMR ($CDCl_3$, 600 MHz): δ = 7.11 (s, 2H, H3, H3′), 5.67 (s, 2H, H8, H8′), 4.24–4.21 (m, 4H, H9$_{eq}$, H9$_{eq}$′, H11$_{eq}$, H11$_{eq}$′), 3.98–3.93 (m, 4H, H9$_{ax}$, H9$_{ax}$′, H11$_{ax}$, H11$_{ax}$′), 3.84 (s, 4H, H6, H6′), 3.31 (s, 4H, H7, H7′), 2.24–2.16 (m, 2H, H10$_{eq}$, H10$_{eq}$′), 1.45–1.42 (m, 2H, H10$_{ax}$, H10$_{ax}$′) ppm. ^{13}C NMR ($CDCl_3$, 150 MHz): δ = 144.5 (o, C5, C5′), 142.4 (o, C2, C2′), 136.4 (m, o, C12, C12′), 124.4 (+, C3, C3′), 123.4 (o, C4, C4′), 117.7–114.1 (m, o, C13, C13′), 111.1–110.8 (m, o, C14), 97.7 (+, C8, C8′), 67.9 (−, C6, C6′), 67.3 (−, C9, C9′, C11, C11′), 58.0 (+, C7, C7′), 25.4 (−, C10,

 © 2023 The Author(s). Published by the Royal Society of Chemistry

Open Access Article. Published on 29 August 2023. Downloaded on 11/8/2025 10:45:24 AM. This article is licensed under a Creative Commons Attribution-NonCommercial 3.0 Unported Licence.

C10′) ppm. IR (ATR): ν = 2966, 2930, 2857, 1736, 1670, 1635, 1564, 1462, 1372, 1339, 1271, 1238, 1191, 1128, 1092, 1019, 976, 913, 855, 734, 641, 581, 550 cm^{-1}. HR-ESI-MS: calc. $[M]^+$: 600.1075, calc. $[M + Na^+]$: 623.0973; found $[M + Na^+]$: 623.0970.

Synthesis of BTE 16

4,4′-(3,3,4,4,5,5-Hexafluorocyclopent-1-en-1,2-diyl)bis(5-(methoxymethyl)thiophene-2-carbaldehyde) (16). 0.232 g (0.39 mmol) of **15c** were dissolved in THF and 10 mL of 2N HCl were added. The reactions mixture was stirred for 4 hours under reflux. After cooling to room temperature 50 mL of a sat. $NaHCO_3$-solution were added. The aqueous phase was extracted with 30 mL diethylether (two times) and the organic phase was washed once with 50 mL of a sat. $NaHCO_3$ solution and four times with 100 mL of water. The organic phase was dried over $MgSO_4$. Removal of the solvent gave the desired product. Yield 0.165 g (88%), light brown oil. ^{1}H NMR ($CDCl_3$, 600 MHz): δ = 9.89 (s, 2H, H6, H6′), 7.74 (s, 2H, H3, H3′), 4.00 (s, 4H, H7, H7′), 3.24 (s, 6H, H8, H8′) ppm. ^{13}C NMR ($CDCl_3$, 150 MHz): δ = 182.0 (+, C6, C6′), 153.8 (o, C5, C5′), 143.5 (o, C2, C2′), 135.3 (+, C3, C3′), 136.5–136.2 (m, o, C9, C9′), 124.2 (o, C4, C4′), 1174–113.7 (m, o, C10, C10′), 110.6 (m, o, C11), 68.3 (−, C7, C7′), 58.8 (−, C8, C8′) ppm. IR (ATR): ν = 2932, 2827, 1732, 1672, 1547, 1452, 1336, 1267, 1227, 1194, 1130, 1097, 1021, 975, 867, 762, 665, 581, 553, 498 cm^{-1}. HR-ESI-MS: calc. $[M]^+$: 484.0238, calc. $[M + Na^+]$: 507.0135; found $[M + Na^+]$: 507.0130.

Synthesis of BTE 22

(4-Bromothiophene-2-yl)methanol (17). Following method (D) a sample of 5.000 g (26.17 mmol) of 4-bromothiophene-2-carbaldehyde **9** and 0.495 g (13.09 mmol) of sodium borohydride were reacted. Yield 5.058 g (99%), yellow-green liquid. ^{1}H NMR ($CDCl_3$, 400 MHz): δ = 7.17–7.16 (m, 1H, H5), 6.91–6.90 (m, 1H, H3), 4.76–4.75 (m, 2H, H6) ppm. The spectroscopic data agree with the literature.[21]

((4-Bromothiophene-2-yl)methoxy)(*tert*-butyl)dimethylsilane (18). A sample of 5.060 g (26.21 mmol) of (4-bromothiophene-2-yl)methanol **17** was dissolved in anhydrous DCM. 3.925 g (57.66 mmol) of 1*H*-imidazole and 4.740 g (31.45 mmol) of TBSCl were added slowly at 0 °C. The reaction mixture was stirred for 30 min at 0 °C and then for 30 min at room temperature. The reaction was then quenched with sat. ammonium chloride solution. The aqueous phase was extracted with 50 mL diethyl ether (two times). The combined organic phases were once washed with 50 mL of 1M HCl, twice with 50 mL water and once with 50 mL of brine. The organic phase was dried over $MgSO_4$ and the solvent was removed *in vacuo*. Yield 5.058 g (99%), yellow liquid. ^{1}H NMR ($CDCl_3$, 400 MHz): δ = 7.11–7.12 (m, 1H, H5), 6.82–6.83 (m, 1H, H3), 4.82 (m, 2H, H6), 0.93 (s, 9H, H9), 0.11 (s, 6H, H7) ppm. The spectroscopic data agree with the literature.[35]

3-Bromo-5-((*tert*-butyl(dimethyl)silyl)oxy)methylthiophene-2-carbaldehyde (19). Following method (C) 4.49 mL (31.98 mmol) of DIPA, 11.50 mL (29.30 mmol) of *n*-BuLi (24% in cyclohexane), 8.191 g (26.65 mmol) of ((4-bromothiophene-2yl)methoxy)(*tert*-butyl)dimethylsilane **18** and 2.46 mL (31.98 mmol) of DMF were reacted. Yield 8.500 g (95%), yellow solid. Mp.: 41 °C. ^{1}H NMR ($CDCl_3$, 600 MHz): δ = 9.91 (s, 1H, H6), 6.94 (s, 1H, H4), 4.78 (s, 2H, H7), 0.93 (s, 9H, H10), 0.12 (s, 6H, H8) ppm. ^{13}C NMR ($CDCl_3$, 150 MHz): δ = 183.1 (+, C6), 157.1 (o, C5), 135.3 (o, C2), 127.0 (+, C4), 121.1 (o, C3), 60.9 (−, C7), 25.9 (+, C10), 18.4 (o, C9), −5.3 (+, C8) ppm. IR (ATR): ν = 2955, 2928, 2884, 2856, 2801, 1652, 1514, 1471, 1446, 1368, 1308, 1251, 1224, 1182, 1130, 1090, 1005, 939, 833, 775, 734, 693, 666, 617, 575, 490 cm^{-1}. HR-ESI-MS: calc. $[M]^+$: 334.0058, calc. $[M + Na^+]$: 356.9951; found $[M + Na^+]$: 356.9926.

(3-Bromo-5-(((*tert*-butyl(dimethyl)silyl)oxy)methyl)thiophen-2-yl)methanol (20). According to method (D) 4.000 g (11.93 mmol) of (3-bromo-5-(*tert*-butyl(dimethyl)silyl)-oxy)methylthiophene-2-carbaldehyde **19** and 0.226 g (5.96 mmol) of sodium borohydride were reacted. Yield 4.024 g (97%), yellow liquid. ^{1}H NMR ($CDCl_3$, 600 MHz): δ = 6.75 (s, 1H, H4), 4.77 (s, 2H, H7), 4.71 (s, 2H, H6), 0.92 (s, 9H, H10), 0.10 (s, 6H, H8) ppm. ^{13}C NMR ($CDCl_3$, 150 MHz): δ = 144.4 (o, C5), 136.0 (o, C2), 125.1 (+, C4), 106.9 (o, C3), 59.7 (−, C7), 58.2 (−, C6), 24.9 (+, C10), 17.4 (o, C9), −6.2 (+, C8) ppm. IR (ATR): ν = 3388, 2954, 2929, 2884, 2856, 1542, 1471, 1462, 1373, 1315, 1254, 1182, 1157, 1123, 1075, 1006, 971, 939, 908, 833, 776, 731, 686, 666 cm^{-1}. HR-ESI-MS: calc. $[M]^+$: 336.0215, calc. $[M + Na^+]$: 359.0107; found $[M + Na^+]$: 359.0109.

((4-Bromo-5-(methoxymethyl)thiophen-2-yl)methoxy)(*tert*-butyl)dimethylsilane (21). According to method (E) 2.000 g (5.93 mmol) of (3-bromo-5-(((*tert*-butyl(dimethyl)silyl)oxy)methyl)thiophen-2-yl)methanol **20**, 0.284 g (7.11 mmol) of sodium borohydride (60% in paraffine) and 0.41 mL (6.52 mmol) of iodomethane were reacted in anhydrous THF. Yield 2.027 (97%), dark brown liquid. ^{1}H NMR ($CDCl_3$, 600 MHz): δ = 6.76 (s, 1H, H3), 4.80 (s, 2H, H8), 4.55 (s, 2H, H6), 3.39 (s, 3H, H7), 0.92 (s, 9H, H11), 0.10 (s, 6H, H9) ppm. ^{13}C NMR ($CDCl_3$, 150 MHz): δ = 145.9 (o, C2), 134.3 (o, C5), 125.9 (+, C3), 109.1 (o, C4), 68.1 (−, C6), 60.7 (−, C8), 58.1 (+, C7), 26.0 (+, 11), 18.5 (o, C10), −5.2 (+, C9) ppm. IR (ATR): ν = 2953, 2928, 2885, 2856, 1542, 1462, 1371, 1254, 1184, 1128, 1080, 1005, 939, 833, 775, 688, 667, 594, 567 cm^{-1}. HR-ESI-MS: calc. $[M]^+$: 350.0371, calc. $[M + Na^+]$: 373.0264; found $[M + Na^+]$: 373.0267 (Δ = 0.0003).

((3,3,4,4,5,5-Hexafluorocyclopent-1-en-1,2-diyl)bis((5-(methoxymethyl)thien-4,2-diyl)methylenoxy))bis(*tert*-butyl(dimethyl)silane) (22). Following method (F) 2.043 g (5.81 mmol) of ((4-bromo-5-(methoxymethyl)thiophen-2-yl)methoxy)(*tert*-butyl)dimethylsilane **21**, 2.51 mL (6.40 mmol) of *n*-BuLi (24% in cyclohexane) and 0.39 mL (2.91 mmol) of octafluorocyclopentene were reacted. Yield 1.070 g (50%), reddish oil. ^{1}H NMR ($CDCl_3$, 600 MHz): δ = 6.90 (s, 2H, H3, H3′), 4.83 (s, 4H, H8, H8′), 3.88 (s, 4H, H6, H6′), 3.17 (s, 6H, H7, H7′), 0.92 (s, 18H, H11, H11′), 0.10 (s, 12H, H9, H9′) ppm. ^{13}C NMR ($CDCl_3$, 150 MHz): δ = 146.4 (o, C2, C2′), 143.3 (o, C5, C5′), 136.3–136.0 (m, C12, C12′), 123.7 (o, C4, C4′), 122.9 (+, C3, C3′), 117.8–114.2 (m, C13, C13′), 113.1–109.1 (m, C14), 68.2 (−, C6, C6′), 60.8 (−, C8, C8′), 58.2 (+, C7, C7′), 25.9 (+, C11, C11′), 18.4 (o, C10, C10′), −5.2 (+, C9, C9′) ppm. IR (ATR): ν = 2933, 2891, 2859, 1722, 1669, 1465, 1367, 1337, 1258, 1193, 1137, 1084, 1020, 978, 910, 836, 777, 732, 671, 613, 566, 497 cm^{-1}. HR-ESI-MS: calc. $[M]^+$: 716.2280, calc. $[M + Na^+]$: 7.39.2172; found $[M + Na^+]$: 739.2176 (Δ = 0.0004). The NMR

Open Access Article. Published on 29 August 2023. Downloaded on 11/8/2025 10:45:24 AM.
This article is licensed under a Creative Commons Attribution-NonCommercial 3.0 Unported Licence.

spectra of this product contain by-products, as this compound is not stable for a longer period of time.

Synthesis of BTE 23

((3,3,4,4,5,5-Hexafluorocyclopent-1-en-1,2-diyl)bis(5-(methoxymethyl)thien-4,2-diyl))dimethanol (23). A sample of 1.009 g (1.41 mmol) of a freshly prepared sample of BTE **22** was dissolved in 20 mL THF. At 0 °C 1.472 g (5.63 mmol) of TBAF in 10 mL of THF were added slowly. The mixture was stirred for 30 min at 0 °C and another 30 min at room temperature. The reaction was quenched with 50 mL of water. The aqueous phase was extracted twice with 50 mL of diethyl ether. The combined organic phases were once washed with 50 mL of 1M HCl, twice with 100 mL of water and once with 50 mL of brine. The organic phase was dried over $MgSO_4$. Column chromatography (*n*-hexane: EE 1 : 1) gave the product. Yield 0.599 g (87%), orange oil. ^{1}H NMR ($CDCl_3$, 600 MHz): $\delta = 6.96$ (s, 2H, H3, H3′), 4.75 (s, 4H, H8, H8′), 3.91 (s, 4H, H6, H6′), 3.17 (s, 6H, H7, H7′) ppm. ^{13}C NMR ($CDCl_3$, 150 MHz): $\delta = 145.2$ (o, C2, C2′), 143.2 (o, C5, C5′), 136.6–136.2 (m, o, C9, C9′), 124.7 (+, C3, C3′), 123.9 (o, C4, C4′), 117.8–114.2 (m, o, C10, C10′), 113.0–108.8 (m, o, C11), 68.1 (−, C6, C6′), 59.9 (−, C8, C8′), 58.2 (+, C7, C7′) ppm. IR (ATR): $\nu =$ 3373, 2934, 2829, 1635, 1560, 1496, 1455, 1364, 1334, 1268, 1190, 1120, 1087, 1038, 1023, 987, 970, 952, 933, 854, 826, 745, 712, 684, 654, 645, 575, 551, 523, 414 cm^{-1}. HR-ESI-MS: calc. $[M]^+$: 488.0551, calc. $[M + Na^+]$: 511.0443; found $[M + Na^+]$: 511.0446 ($\Delta = 0.0003$).

Author contributions

Thea Weingartz performed all syntheses, spectroscopic characterizations and produced all PMMA films. Sven Nagorny prepared the reference compound and investigated the Hammett–Brown correlations together with Thea Weingartz. André Eitzeroth determined the absorption coefficients and quantum yields. Marvin Schewe constructed the experimental setup and investigated the stabilities of the films. Jörg Adams, Christian Rembe and Andreas Schmidt are group leaders. Together with other cooperation partners (Alexander Egner, Vladimir Belov, Stefan Hell), they have a common project funded by the German Research Foundation (Deutsche Forschungsgemeinschaft DFG), called "NanoVidere – Photochromic Layers for Nanoscopy".

Conflicts of interest

There are no conflicts of interest to declare.

Acknowledgements

The German Research Foundation is gratefully acknowledged for funding these studies (project numbers 504588119 (A. S.) and 412988268 (C. R.)).

Notes and references

1 M. Irie, T. Fukaminato, K. Matsuda and S. Kobatake, *Chem. Rev.*, 2014, **114**, 12174–12277.

2 Recent examples: (*a*) A. Kunz, N. Oberhof, F. Scherz, L. Martins, A. Dreuw and H. A. Wegner, *Chem. –Eur. J.*, 2022, **28**, e202200972; (*b*) F. Gao, Z. Bi, S. Wang, Z. Zhao, Y. Dong and X. Li, *Colloids Surf., A*, 2022, **647**, 129088; (*c*) B. Xu, J. Ding, A. Caliari, N. Lu, F. Han, Y. Xia, J. Xu and T. Yomo, *Biochem. Biophys. Res. Commun.*, 2022, **618**, 113–118.

3 Recent examples: (*a*) H. Zhao, J. Huai, C. Weng and H. Han, *J. Mol. Struct.*, 2022, **1263**, 133146; (*b*) D. Mukherjee, G. Chakraborty, N. Md. Hasan, U. Pal, P. Singh, T. Rakshit, R. I. Alsantali, D. Saha, A. Tanusri, A. Saleh, R. Das and S. K. Pal, *J. Photochem. Photobiol., A*, 2022, **430**, 113958.

4 Recent example: S. Padgaonkar, C. T. Eckdahl, J. K. Sowa, R. Lopez-Arteaga, D. E. Westmoreland, E. F. Woods, S. Irgen-Gioro, B. Nagasing, T. Seideman, M. C. Hersam, J. A. Kalow and E. A. Weiss, *Nano Lett.*, 2021, **21**, 854–860.

5 (*a*) M. Albrecht, M. Gjikaj and A. Schmidt, *Tetrahedron*, 2010, **66**, 7149–7154; (*b*) M. Albrecht, M. Yulikov, T. Kohn, G. Jeschke, J. Adams and A. Schmidt, *J. Mater. Chem.*, 2010, **20**, 3025–3034; (*c*) M. Albrecht, O. Schneider and A. Schmidt, *Org. Biomol. Chem.*, 2009, **7**, 1445–1453; (*d*) A. Schmidt, M. Albrecht, T. Mordhorst, M. Topp and G. Jeschke, *J. Mater. Chem.*, 2007, **17**, 2793–2800.

6 (*a*) K. Matsuda and M. Irie, *J. Photochem. Photobiol., C*, 2004, **5**, 169–182; (*b*) H. Tian and S. Yang, *Chem. Soc. Rev.*, 2004, **33**, 85–97; (*c*) T. J. Wigglesworth, A. J. Myles and N. R. Branda, *Eur. J. Org Chem.*, 2005, 1233–1238; (*d*) C. Yun, J. You, J. Kim, J. Huh and E. Kim, *J. Photochem. Photobiol., C*, 2009, **10**, 111–129; (*e*) M. Irie and M. Morimoto, *Pure Appl. Chem.*, 2009, **81**, 1655–1665; (*f*) T. Tsujioka and M. Irie, *J. Photochem. Photobiol., C*, 2010, **11**, 1–14; (*g*) A. Bianco, S. Perissinotto, M. Garbugli, G. Lanzani and C. Bertarelli, *Laser Photonics Rev.*, 2001, **5**, 711–736; (*h*) C. Bertarelli, A. Bianco, R. Castagna and G. Pariani, *J. Photochem. Photobiol., C*, 2011, **12**, 106–125; (*i*) G. Szalóki and J.-L. Pozzo, *Chem.–Eur. J.*, 2013, **19**, 11124–11132; (*j*) A. Bianchi, E. Delgado-Pinar, E. Garcia-Espana, C. Giorgi and F. Pina, *Coord. Chem. Rev.*, 2014, **260**, 156–215; (*k*) E. C. Harvey, B. L. Feringa, J. G. Vos, W. R. Browne and M. T. Pryce, *Coord. Chem. Rev.*, 2015, **282–283**, 77–86; (*l*) A. Fihey, A. Perrier, W. R. Browne and D. Jacquemin, *Chem. Soc. Rev.*, 2015, **44**(11), 3719–3759; (*m*) C. Xiao, W.-Y. Zhao, D.-Y. Zhou, Y. Huang, Y. Tao, W.-H. Wu and C. Yang, *Chin. Chem. Lett.*, 2015, **26**(7), 817–824; (*n*) M. Irie, *Pure Appl. Chem.*, 2015, **87**(7), 617–626; (*o*) S.-Z. Pu, Q. Sun, C.-B. Fan, R.-J. Wang and G. Liu, *J. Mater. Chem. C*, 2016, **4**(15), 3075–3093; (*p*) A. G. Lvov and V. Z. Shirinyan, *Chem. heterocycl. compounds*, 2016, **52**(9), 658–665; (*q*) L.-N. Fu, B. Leng, Y.-S. Li and S.-K. Gao, *Chin. Chem. Lett.*, 2016, **27**(8), 1319–1329; (*r*) S.-L. Huang, T. S. A. Hor and G.-X. Jin, *Coord. Chem. Rev.*, 2017, **346**, 112–122.

7 (*a*) M. Herder, B. M. Schmidt, L. Grubert, M. Paetzel, J. Schwarz and S. Hecht, *J. Am. Chem. Soc.*, 2015, **137**, 2738–2747; (*b*) M. Irie, T. Lifka, K. Uchida, S. Kobatake and Y. Shindo, *Chem. Commun.*, 1999, 747–750; (*c*) T. Hirose, Y. Inoue, J.-y. Hasegawa, K. Higashiguchi and K. Matsuda, *J. Phys. Chem. A*, 2014, **118**, 1084–1093; (*d*) E. C. Harvey,

 © 2023 The Author(s). Published by the Royal Society of Chemistry

Open Access Article. Published on 29 August 2023. Downloaded on 11/8/2025 10:45:24 AM.
This article is licensed under a Creative Commons Attribution-NonCommercial 3.0 Unported Licence.

J. Areephong, A. A. Cafolla, C. Long, W. R. Browne, B. L. Feringa and M. T. Pryce, *Organometallics*, 2014, **33**, 447–456; (*e*) T. Sakano, Y. Imaizumi, T. Hirose and K. Matsuda, *Chem. Lett.*, 2013, **42**, 1537–1539; (*f*) H. Shoji and S. Kobatake, *Chem. Commun.*, 2013, **49**, 2362–2364.

8 (*a*) H. Wang, H. Lin, W. Xu and D. Zhu, *Chem. –Eur. J.*, 2013, 3366–3373; (*b*) H. Lin, W. Xu and D. B. Zhu, *J. Mater. Chem.*, 2010, **20**, 884–890; (*c*) S. Kobatake, U. Kingo, E. Tsuchida and M. Irie, *Chem. Commun.*, 2002, 2804–2805; (*d*) K. Uchida, E. Tsuchida, Y. Aoi, S. Nakamura and M. Irie, *Chem. Lett.*, 1999, **63**, 64; (*e*) M. Irie, *Chem. Rev.*, 2000, **100**, 1685–1716; (*f*) K. Morimitsu, S. Kobatake and M. Irie, *Tetrahedron Lett.*, 2004, **45**, 1155–1158.

9 S. Nagorny, F. Lederle, V. Udachin, T. Weingartz, E. G. Hübner, S. Dahle, W. Maus-Friedrichs, J. Adams and A. Schmidt, *Eur. J. Org Chem.*, 2021, 3178–3189.

10 S. Kobatake, Y. Terakawa and H. Imagawa, *Tetrahedron*, 2009, **65**, 6104–6108.

11 (*a*) S. Fukumoto, T. Nakashima and T. Kawai, *Eur. J. Org Chem.*, 2011, 5047–5053; (*b*) S. Fukumoto, T. Nakashima and T. Kawai, *Angew. Chem., Int. Ed.*, 2011, **50**, 1565–1568; (*c*) W. Li, C. Jiao, X. Li, Y. Xie, K. Nakatani, H. Tian and W. Zhu, *Angew. Chem., Int. Ed.*, 2014, **53**, 4603–4607.

12 (*a*) Y. Ishibashi, H. Miyasaka, S. Kobatake, M. Irie and Y. Yokoyama, *Pacific Rim Conference on Lasers and Electrooptic*, 2007, vol. 1–4, p. 1364; (*b*) Y. Ishibashi, M. Mukaida, M. Falkenstrom, H. Miyasaka, S. Kobatake and M. Irie, *Phys. Chem. Chem. Phys.*, 2009, **11**, 2640–2648; (*c*) Y. Ishibashi, K. Okuno, C. Ota, T. Umesato, T. Katayama, M. Murakami, S. Kobatake, M. Irie and H. Miyasaka, *Photochem. Photobiol. Sci.*, 2010, **9**, 172–180; (*d*) S. P. Aloïse, M. Sliwa, Z. Pawlowska, J. Réhault, J. Dubois, O. Poizat, G. Buntinx, A. Perrier, F. Maurel and S. Yamaguchi, *J. Am. Chem. Soc.*, 2010, **132**, 7379–7390.

13 (*a*) S.-J. Lim, B.-K. An and S. Y. Park, *Macromolecules*, 2005, **38**, 6236–6239; (*b*) A. Fernandez and J.-M. Lehn, *Adv. Mater.*, 1998, **10**, 1519–1522; (*c*) T. Kawai, T. Sasaki and M. Irie, *Chem. Commun.*, 2001, 711–712; (*d*) A. Osuka, D. Fujikane, H. Shinmori, S. Kobatake and M. Irie, *J. Org. Chem.*, 2001, **66**, 3913–3923; (*e*) K. Yagi, C. F. Soong and M. Irie, *J. Org. Chem.*, 2001, **66**, 5419–5423; (*f*) T. B. Norsten and N. R. Branda, *J. Am. Chem. Soc.*, 2001, **123**, 1784–1785; (*g*) B. Chen, M. Wang, Y. Wu and H. Tian, *Chem. Commun.*, 2002, **1060**, 1061; (*h*) M. Irie, T. Fukaminato, T. Sasaki, N. Tamai and T. Kawai, *Nature*, 2002, **420**, 759–760; (*i*) S. Murase, M. Teramoto, H. Furukawa, Y. Miyashita and K. Horie, *Macromolecules*, 2003, **36**, 964–966; (*j*) G. Pariani, R. Castagna, R. Menon, C. Bertarelli and A. Bianco, *Opt. Lett.*, 2013, **38**, 3024–3027.

14 T. Ago, T. Kubota and H. Fukumoto, 2020, JP2020050618.

15 (*a*) M. Irie, T. Lifka, K. Uchida, S. Kobatake and Y. Shindo, *Chem. Commun.*, 1999, 747–750; (*b*) T. Hirose, Y. Inoue, J.-y. Hasegawa, K. Higashiguchi and K. Matsuda, *J. Phys. Chem. A*, 2014, **118**, 1084–1093; (*c*) E. C. Harvey, J. Areephong, A. A. Cafolla, C. Long, W. R. Browne, B. L. Feringa and M. T. Pryce, *Organometallics*, 2014, **33**, 447–456; (*d*) T. Sakano, Y. Imaizumi, T. Hirose and K. Matsuda, *Chem. Lett.*, 2013, **42**, 1537–1539; (*e*) H. Ikeda, A. Sakai, A. Kawabe, H. Namai and K. Mizuno, *Tetrahedron Lett.*, 2008, **49**, 4972–4976; (*f*) G. Sevez, J. Gan, J. Pan, X. Sallenave, A. Colin, H. Saadoui, A. Saleh, F. Vögtle and J.-L. Pozzo, *J. Phys. Org. Chem.*, 2007, **20**, 888–893; (*g*) A. Peters and N. R. Branda, *Adv. Mater. Opt. Electron.*, 2000, **10**, 245–249; (*h*) K. Higashiguchi, K. Matsuda, S. Kobatake, T. Yamada, T. Kawai and M. Irie, *Bull. Chem. Soc. Jpn.*, 2000, **73**, 2389–2394.

16 (*a*) H. Shoji and S. Kobatake, *Chem. Commun.*, 2013, **49**, 2362–2364; (*b*) H.-H. Liu and Y. Chen, *New J. Chem.*, 2012, **36**, 2223–2227; (*c*) K. Higashiguchi, K. Matsuda, T. Yamada, T. Kawai and M. Irie, *Chem. Lett.*, 2000, **29**, 1358–1359.

17 (*a*) K. Uno, M. L. Bossi, M. Irie, V. N. Belov and S. W. Hell, *J. Am. Chem. Soc.*, 2019, **141**, 16471–16478; (*b*) C. Zheng, S. Pu, J. Xu, M. Luo, D. Huang and L. Shen, *Tetrahedron*, 2007, **63**, 5437–5449.

18 I. E. Nifant'ev, A. A. Vinogradov, A. V. Churakov, V. V. Bagrov, I. A. Kashulin, V. A. Roznyatovsky, Y. K. Grishin and P. V. Ivchenko, *Appl. Catal., A*, 2019, **571**, 12–24.

19 M. Manuela, M. Raposo, C. Herbivo, V. Hugues, G. Clermont, M. C. R. Castro, A. Comel and M. Blanchard-Desce, *Eur. J. Org Chem.*, 2016, **2016**, 5263–5273.

20 M. Fukagawa, I. Kawamura, T. Ubukata and Y. Yokoyama, *Chem. –Eur. J.*, 2013, **19**, 9434–9437.

21 C. Jagusch, M. Negri, U. E. Hille, Q. Hu, M. Bartels, K. Jahn-Hoffmann, M. A. P.-B. Mendieta, B. Rodenwaldt, U. Müller-Vieira, D. Schmidt, T. Lauterbach, M. Recanatini, A. Cavalli and R. W. Hartmann, *Bioorg. Med. Chem.*, 2008, **16**, 1992–2010.

22 S. P. Langston, S. Grossman, D. England, R. Afroze, N. Bence, D. Bowman, N. Bump, R. Chau, B.-C. Chuang, C. Claiborne, L. Cohen, K. Connolly, M. Duffey, N. Durvasula, S. Freeze, M. Gallery, K. Galvin, J. Gaulin, R. Gershman, P. Greenspan, J. Grieves, J. Guo, N. Gulavita, S. Hailu, X. He, K. Hoar, Y. Hu, Z. Hu, M. Ito, M.-S. Kim, S. W. Lane, D. Lok, A. Lublinsky, W. Mallender, C. McIntyre, J. Minissale, H. Mizutani, M. Mizutani, N. Molchinova, K. Ono, A. Patil, M. Qian, J. Riceberg, V. Shindi, M. D. Sintchak, K. Song, T. Soucy, Y. Wang, H. Xu, X. Yang, A. Zawadzka, J. Zhang and S. M. Pulukuri, *J. Med. Chem.*, 2021, **64**, 2501–2520.

23 (*a*) C. Reichardt, *Solvent and Solvent Effects in Organic Chemistry*, Wiley-VCH, 2003, vol. 3; (*b*) C. Reichardt and R. Müller, *Liebigs Ann. Chem.*, 1976, 1937–1952; (*c*) H. Wamhoff and A. Schmidt, *J. Org. Chem.*, 1993, **58**, 6976–6984; (*d*) C. Reichardt and W. Grahn, *Chem. Ber.*, 1970, **103**, 1072–1087; (*e*) E. M. Kosower, D. Hofmann and K. Wallenfels, *J. Am. Chem. Soc.*, 1962, **84**, 2755–2757.

24 (*a*) L. P. Hammett, *J. Am. Chem. Soc.*, 1937, **59**, 96–103; (*b*) L. P. Hammett, *Trans. Faraday Soc.*, 1938, **34**, 156–165; (*c*) H. H. Jaffé, *Chem. Rev.*, 1953, **53**, 191–261; (*d*) O. Exner, *Adv. Linear Free Energy Relat.*, ed. N. B. Chapman, 1972, pp. 1–69; (*e*) C. Hansch, A. Leo and R. W. Taft, *Chem. Rev.*, 1991, **91**, 165–195.

25 M. B. Smith, *March's Advanced Organic Chemistry*, Wiley, 7th edn, 2013, pp. 352–355.

Open Access Article. Published on 29 August 2023. Downloaded on 11/8/2025 10:45:24 AM.
This article is licensed under a Creative Commons Attribution-NonCommercial 3.0 Unported Licence.

26 (*a*) Y. Okamoto, T. Inukai and H. C. Brown, *J. Am. Chem. Soc.*, 1958, **80**, 4979–4987; (*b*) J. Shorter, *Chem. Unserer Zeit*, 1985, **19**, 197–208.
27 S. Nagorny, T. Weingartz, J. C. Namyslo, J. Adams and A. Schmidt, *Eur. J. Org Chem.*, 2023, **26**, e202200996.
28 S. Kobatake, T. Yamada, K. Uchida, N. Kato and M. Irie, *J. Am. Chem. Soc.*, 1999, **121**, 2380–2386.
29 (*a*) Q.-T. Fu, X. Yan, T. Li, X.-Y. Zhang, Y. He, W.-D. Zhang, Y. Liu, Y. Li and Z.-G. Gu, *New J. Chem.*, 2019, **43**, 15797–15803; (*b*) U. Ali, K. J. B. A. Karim and N. A. Buang, *Polym. Rev.*, 2015, **55**, 678–705.
30 M. Maafi, *Molecules*, 2008, **13**, 2260–2302.
31 K. Stranius and K. Börjesson, *Sci. Rep.*, 2017, **7**, 41145.
32 H. Zhao, J. W. Dankwardt, S. G. Koenig and S. P. Singh, *Tetrahedron Lett.*, 2012, **53**, 166–169.
33 E. Kianmehr, M. Fardpour and K. M. Khan, *Eur. J. Org Chem.*, 2017, **18**, 2661–2668.
34 A. de Meijere, L. Zhao, V. N. Belov, M. Bossi, M. Noltemeyer and S. W. Hell, *Chem. –Eur. J.*, 2007, **13**, 2503–2516.
35 S. Thayumanavan, J. Mendez and S. R. Marder, *J. Org. Chem.*, 1999, **64**, 4289–4297.

 © 2023 The Author(s). Published by the Royal Society of Chemistry